



U.S. DEPARTMENT OF
ENERGY

PNNL-20796

Prepared for the U.S. Department of Energy
under Contract DE-AC05-76RL01830

FY2011 Annual Report for the Actinide Isomer Detection Project

GA Warren
CJ Francy
JJ Ressler¹

LE Erikson
G Tatishvili
R Hatarik¹

¹ Lawrence Livermore National Laboratory

October 2011



Pacific Northwest
NATIONAL LABORATORY

*Proudly Operated by **Battelle** Since 1965*

DISCLAIMER

This report was prepared as an account of work sponsored by an agency of the United States Government. Neither the United States Government nor any agency thereof, nor Battelle Memorial Institute, nor any of their employees, makes **any warranty, express or implied, or assumes any legal liability or responsibility for the accuracy, completeness, or usefulness of any information, apparatus, product, or process disclosed, or represents that its use would not infringe privately owned rights.** Reference herein to any specific commercial product, process, or service by trade name, trademark, manufacturer, or otherwise does not necessarily constitute or imply its endorsement, recommendation, or favoring by the United States Government or any agency thereof, or Battelle Memorial Institute. The views and opinions of authors expressed herein do not necessarily state or reflect those of the United States Government or any agency thereof.

PACIFIC NORTHWEST NATIONAL LABORATORY

operated by

BATTELLE

for the

UNITED STATES DEPARTMENT OF ENERGY

under Contract DE-AC05-76RL01830

Printed in the United States of America

Available to DOE and DOE contractors from the
Office of Scientific and Technical Information,
P.O. Box 62, Oak Ridge, TN 37831-0062;
ph: (865) 576-8401
fax: (865) 576-5728
email: reports@adonis.osti.gov

Available to the public from the National Technical Information Service,
U.S. Department of Commerce, 5285 Port Royal Rd., Springfield, VA 22161
ph: (800) 553-6847
fax: (703) 605-6900
email: orders@ntis.fedworld.gov
online ordering: <http://www.ntis.gov/ordering.htm>



This document was printed on recycled paper.

(9/2003)

FY2011 Annual Report for the Actinide Isomer Detection Project

GA Warren LE Erikson
CJ Francy G Tatishvili
JJ Ressler¹ R Hatarik¹

October 2011

Prepared *for the* U. S. DEPARTMENT OF ENERGY
under Contract DE-AC05-76RL01830

Pacific Northwest National Laboratory
Richland, WA 99354

¹Lawrence Livermore National Laboratory

Executive Summary

This project seeks to identify a new signature for actinide element detection in active interrogation. This technique works by exciting and identifying long-lived nuclear excited states (isomers) in the actinide isotopes and/or primary fission products. Observation of isomers in the fission products will provide a signature for fissile material. For the actinide isomers, the decay time and energy of the isomeric state is unique to a particular isotope, providing an unambiguous signature for SNM.

This project entails isomer identification and characterization and neutron population studies. This document summarizes activities from its third year – completion of the isomer identification characterization experiments and initialization of the neutron population experiments.

The population and decay of the isomeric state in ^{235}U remains elusive, although a number of candidate gamma rays have been identified in earlier work. In the course of the experiments, a number of fission fragment isomers were populated and measured [Ressler 2010]. The decays from these isomers may also provide a suitable signature for the presence of fissile material.

Several measurements were conducted throughout this project. This report focuses on the results of an experiment conducted collaboratively by PNNL, LLNL and LBNL in December 2010 at LBNL. The measurement involved measuring the gamma-rays emitted from an HEU target when bombarded with 11 MeV neutrons. This report discussed the analysis and resulting conclusions from those measurements.

There was one candidate, at 1164.9 keV, of an isomeric signature of ^{235}U . The half-life of the state is estimated to be 42 μs . The measured time dependence fits the decay time structure, however the statistics of the measurement prevent the ambiguous declaration that the gamma-ray has the anticipated time structure. Preliminary investigations into alternative explanations of this gamma line, i.e. fission products, neutron scattering, neutron absorption and room background, did not support those alternative origins. In order to unambiguously declare the 1164-keV gamma ray a signature of isomeric transition of ^{235}U , a measurement with more statistic and better systematic controls would be necessary..

Acronyms and Initialisms

ADC	Analog-to-Digital Converter
FWHM	Full-width-at-half-maximum
HEU	Highly Enriched Uranium
HPGe	High-Purity Germanium
LBNL	Lawrence Berkeley National Laboratory
LLNL	Lawrence Livermore National Laboratory
PNNL	Pacific Northwest National Laboratory
SNM	Special Nuclear Materials
TAC	Time-to-Amplitude Converter
TDC	Time to Digital Converter
DU	Depleted uranium

Contents

Executive Summary	ii
Acronyms and Initialisms.....	iii
Contents	iv
1.0 Introduction.....	1
2.0 Experimental Setup	1
2.1 Beam Line.....	1
2.2 Targets	2
2.3 Detectors	3
3.0 Calibrations	5
3.1 Time Calibrations	5
3.2 Energy calibrations	5
3.3 Beam status	5
3.4 Live Time Correction.....	6
4.0 Analysis.....	7
4.1 Time Dependence	7
4.2 Gamma Peak Fit Procedure	8
4.3 Time Structure Identification.....	10
5.0 Conclusion	12
6.0 References.....	13

1.0 Introduction

This project seeks to identify a new signature for actinide element detection in active interrogation. This technique works by exciting and identifying long-lived nuclear ($\sim 10 - 100 \mu\text{s}$) excited states (isomers) in the actinide isotopes and/or primary fission products. Observation of isomers in the fission products will provide a new signature for fissile material. For the actinide isomers, the decay time and energy of the isomeric state is unique to a particular isotope, providing an unambiguous signature for special nuclear materials (SNM).

The high-energy gamma rays emitted from the actinide isomer decay allow the photon emission to be easily identifiable for two reasons. First, the gamma-ray background is low at the expected isomeric decay energy (2-3 MeV). Second, this energy is the least attenuated through any material. Moreover, the emission of isomeric decay photons will fall within an optimal time window between the end of the neutron pulse and the onset of gamma rays arising from neutron-induced beta decay products. The unique characteristics of the high energy and fast decay time for the actinide isomers provide an unambiguous signature for the emitting isotope. The scientific background for this new signature is described in *Annual Progress Report for Actinide Isomer Detection (2009)* [Ressler 2009].

This effort was proposed to search for the actinide isomers, with a focus on ^{235}U . In the first year, experiments were conducted to characterize actinide isomers of interest [Ressler 2008]. Several candidate signatures of ^{235}U isomers were identified, although the results were not conclusive. The second year, analysis was completed on the characterization measurements and neutron population experiments were initiated. The third year, the neutron population measurements at Lawrence Berkeley National Laboratory (LBNL) at the 88" cyclotron were completed. Unfortunately, there were significant issues with the measurements that limited the conclusions that could be drawn. As a result, in early FY2011, a second set of measurements at LBNL was completed.

This report covers the progress of the progress completed in FY2011. It will discuss the measurements at LBNL, the analysis of the resulting data, and then the conclusions drawn.

2.0 Experimental Setup

2.1 Beam Line

The experiment was conducted at the 88" cyclotron facility at LBNL in December 2010. A deuteron beam struck a thick tantalum disk with a copper backing in the cyclotron vault (see Figure 2-1). Neutrons from the break-up reaction were emitted into experimental Cave 0. The detectors and target were set up in Cave 0/2 as previous test measurements demonstrated a significantly lower background compared to Cave 0/1. A liquid scintillator (BC 501-A from Saint Gobain) were placed down stream of the target and detectors and used to monitor the neutron beam. The liquid scintillator was $\sim 11 \text{ cm}^2$. It was placed at 0° relative to the neutron beam axis and was used to monitor the beam pulsing and neutron flux. The liquid scintillator employed pulse-shape discrimination to delineate between photon and neutron events.

Deuterons at 25 MeV were used to produce neutrons of approximately 11.4 MeV. This energy covers the peak of the $^{235}\text{U}(n,2n)^{234}\text{U}$ cross section, as well as $^{235}\text{U}(n,f)$. The broad energy spread of the neutron

energy distribution will also likely cover the expected peak for the ^{235}U isomeric (n,n') state. The inelastic isomer population is expected to peak near 8 MeV neutron energy. The beam was pulsed at 50 μs , with a 50% duty cycle. This time structure provides a maximum sensitivity to isomeric decays with 10 to 20- μs half-lives.

The experiment was scheduled for 40 hours of beam time, but only 33 hours were delivered to the target due to a combination of extended beam tuning and experiment preparation. Initially, the experiment started with 100 nA of deuteron beam on target, but over time the beam current was increased to 2.1 to 2.2 μA . This increase was enabled by a reevaluation of the safety criteria.

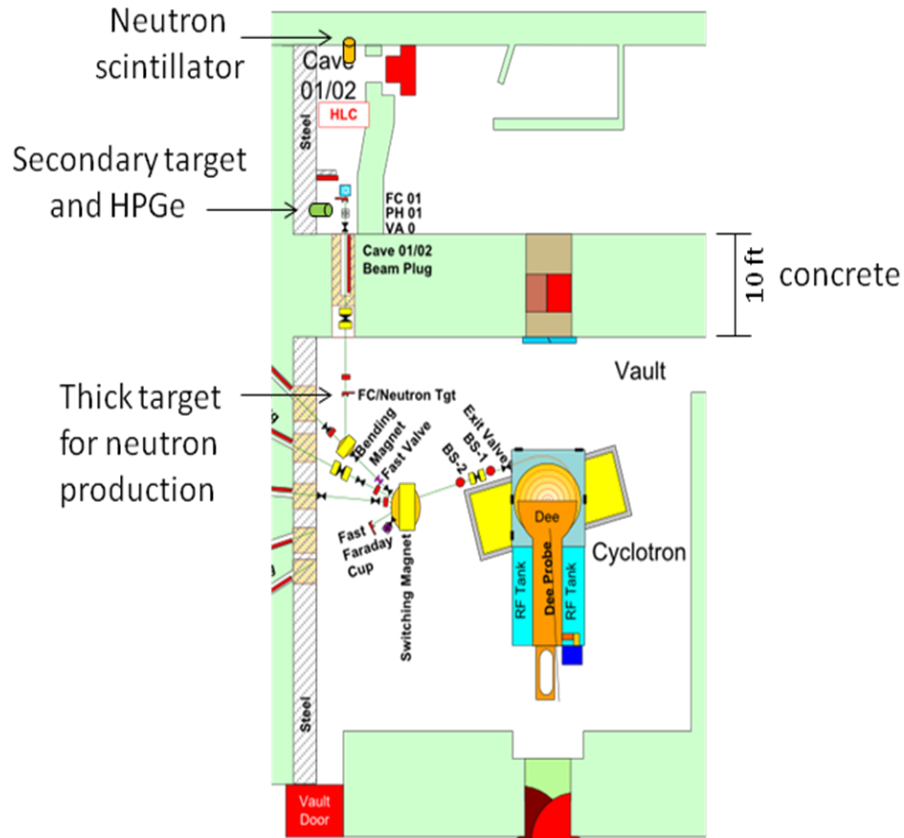


Figure 2-1: Diagram of the cyclotron and experimental facility for the LBNL measurements. The measurement rooms, Cave 0/1 and Cave 0/2, are in the upper left corner of the diagram. For this measurement, the HPGe were placed in Cave 0/2 just outside the wall of the Cave 0/1, contrary to this figure.

2.2 Targets

The HEU target was prepared by PNNL and consisted of 0.4905 g of 99.89% enriched uranium. It consisted of one-and-a-half circles of uranium metal. Each circle was ~5 mils thick, about $\frac{1}{2}$ " in diameter, and weighed 0.327 g. The isotopics of the HEU are as shown in Table 2-1.

Table 2-1: Isotopic Mass of HEU Sample

Isotope	%Mass
^{235}U	99.89%
^{234}U	0.035%
^{236}U	0.025%
^{238}U	0.053%

The target holder consisted of three pieces (Figure 2-2). A structure frame in the shape of football “goal posts,” foil that wrapped around the HEU, and wire that suspended the foil between the goal posts of the frame. Iron was selected as the material for the target holder. Iron does not activate easily, and it provides a strong “beam-on” signal through inelastic neutron excitation reactions.

**Figure 2-2:** HEU target from PNNL

The HEU was packaged in two sets of metal foils of 99% iron that were 0.025 mm thick. The inner set of foils was made of two 2" squares of the foil welded to form four quadrants – each opening out on two adjacent sides and welded closed on the other two sides. The circle and half-circle of the HEU were inserted into two adjacent quadrants of the inner set of foils. The inner foils were then placed inside a set of outer foils. The outer foils were shaped by starting with a 2-inch “ribbon” of foil, folding over on itself from both ends with the middle portion extending outward on one side wider than the rest of the loop of foil. The bottom and top portion of the outer foils were welded horizontally and along one of the vertical sides, leaving an opening for inserting the HEU-filled inner foils. The two ends of the ribbon of the outer foils were welded in such a way as to leave room for the iron wire to be threaded through them to be attached to the posts of the structural frame.

The iron wire is 99.99% pure iron and is 0.020" in diameter. The goal-post frame was machined out of solid pieces of A36 ASTM A1018 SS GR 36 Type 2 Structural Steel, 10" x 10" x ¼". The HEU target was not removed from the plastic bag during the measurement.

2.3 Detectors

Photons were detected in three large-volume HPGe clover detectors and a 130% relative efficiency HPGe detector. Clover detectors are comprised of four close-packed crystals of ~25% efficiency each. The 130% detector was a p-type semi-coaxial crystal with a transistor reset preamplifier. The detectors were

arranged at two levels, one slightly above and one slightly below beam height. Two detectors were placed on each level, as shown in Figure 2-3. The detectors were placed close to the target at $\sim 70^\circ$ and $\sim 110^\circ$ with respect to the beam.



Figure 2-3: Detector and target setup for the run.

Data was recorded using a VME-based data acquisition system. Signals from the detectors were split and routed to record time and energy information using a TDC and ADC, respectively. Also, the number of pulses was counted with a scaler. Unfortunately, the TDC did not span an adequate range of times for these measurements, so that its information is not helpful. In addition to the TDC, the timing of the detector signal was measured using a Time-to-Amplitude Converter (TAC) and ADC. There was one TAC signal per detector, so that any leaf on a clover would stop the TAC for that detector.

The TAC-ADC approach is capable of reading the time for a single event within a gate, which is somewhat limited. Initially, the TAC-ADC system was setup for common-stop mode, in which the time of the detector signal starts the TAC and the closing of the event gate stops the TAC. Unfortunately, the implementation was imperfect, resulting in the loss of significant information. For the last few hours of the measurement, the TAC was switched to common-start mode, in which the beam-off signal was used to start the TAC and the discriminated detector signals were used to stop the TAC. Reliable timing information from the detectors was acquired in this mode.

A sample histogram of the timing signal generated by the TAC is shown in Figure 2-4. There are two primary features to this histogram. The histogram can be divided roughly into four separate regions. Those regions coincide with whether the beam is on or off. The first region on the left is beam off, the second is beam on, and so forth. The detector rates are noticeably elevated for the beam-on sections. The second feature is the exponential decay of the histogram. This exponential falloff is due to the single-hit nature of the TAC; if an event occurs earlier in the time window then the TAC is not available to record the next event.

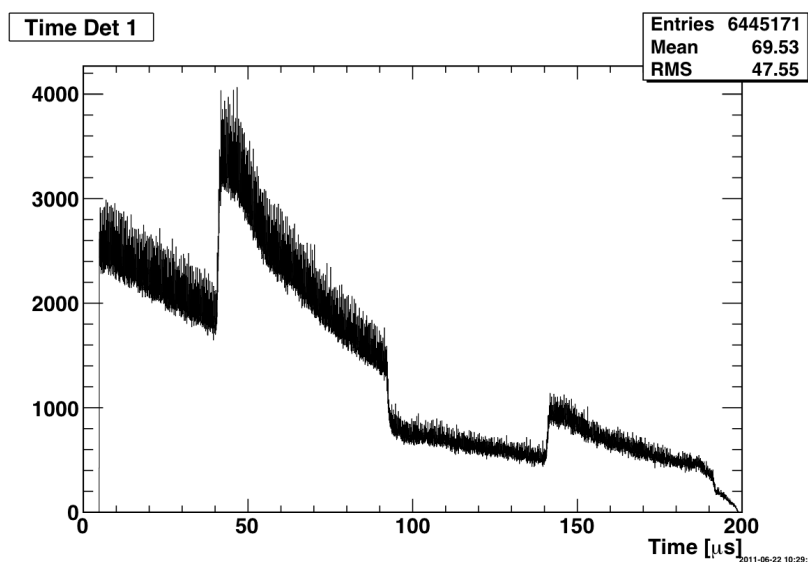


Figure 2-4: Histogram of time distribution from one of the clover detectors.

3.0 Calibrations

3.1 Time Calibrations

The TAC-ADC timing information was calibrated following a well-established procedure. A signal with variable delay relative to the start gate of the TAC was sent to the stop of the TAC. The TAC-ADC readings were then recorded for a series of known time differences between the start and stop signals. This information was then used in the off-line analysis to convert from ADC channel to time.

3.2 Energy calibrations

The gains of the HPGe detectors were calibrated using well-known gamma lines. With beam on the HEU target, the strong peaks corresponding to 185.7 from ^{235}U decay, 511.0 keV from pair production, 1332.5 keV from ^{60}Co decay, and 2223.2 keV from neutron capture on protons were used for the calibrations. The ^{60}Co gamma rays are a room contaminant while the ^{235}U gamma rays are from the target. Calibrations were completed for each of the individual data runs and were fairly stable from run to run. The fourth leaf of the first clover detector was ignored in the data analysis because of poor performance.

3.3 Beam status

In the July 2010 measurements, there were complications with the determination of the beam-on/beam-off. This issue was resolved for this measurement. Figure 3-1 is a 2D plot of the beam flag value versus the detector timing; note the logarithmic scale of the Z-axis (color). The high values of the beam flag ADC indicate that the beam is off, while the low ADC values indicate that the beam is on. One must be careful with the interpretation of this plot. It may appear that there are significant anti-correlated events between the beam flag and the detector timing (e.g. beam off according to the beam flag when expect beam on according to the detector timing). However, less than 0.3% of the events are anti-correlated. We conclude that one can use the detector timing information to unambiguously determine the beam status.

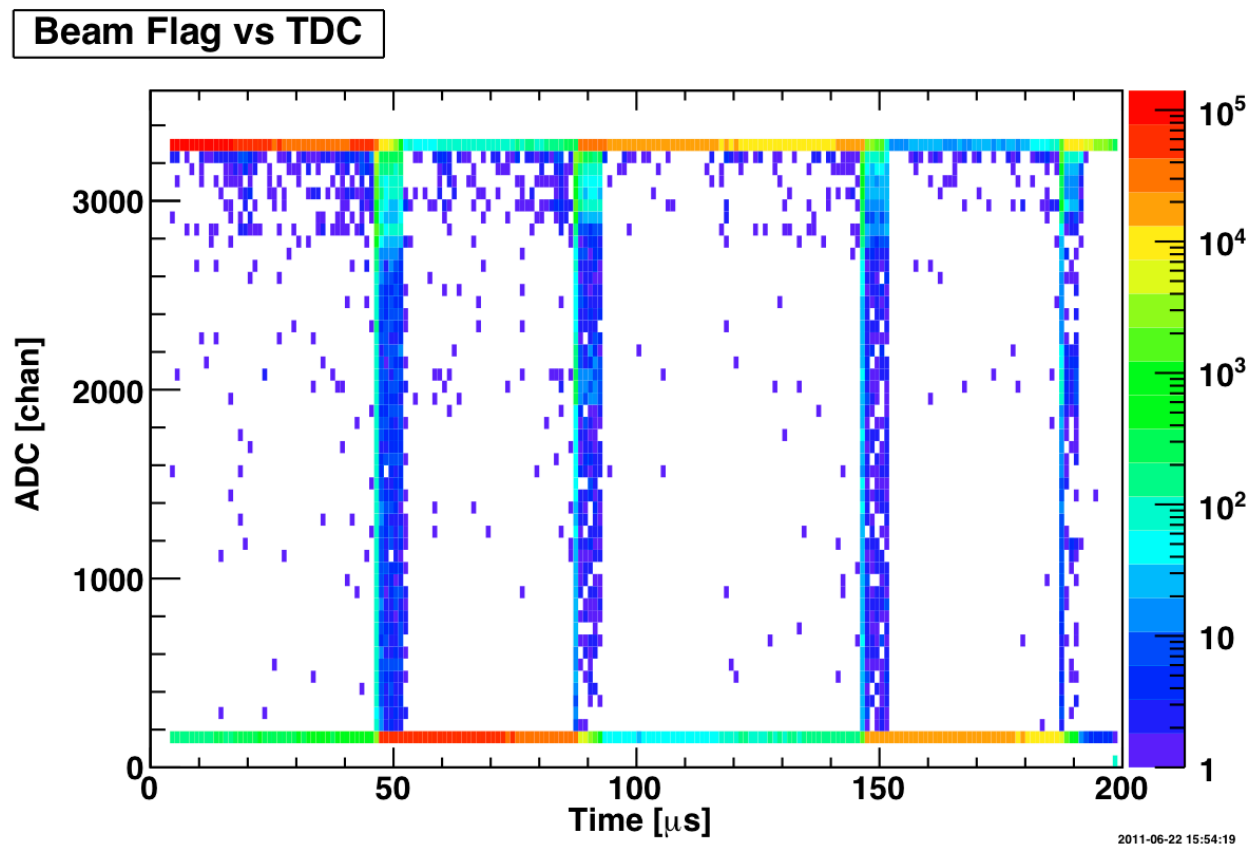


Figure 3-1: Beam flag ADC versus detector #3 timing. Large ADC channels indicate that the beam is off.

3.4 Live Time Correction

It is necessary to correct the time distribution of events using the TACs to account for the effective availability of the system. Once a stop signal has been generated for a TAC, no other timing information will be recorded until the TAC is reset. As a result, this single-hit nature of the TAC means that the system is unavailable for the later events, which creates an exponential decay in the timing histogram as shown in Fig. 2-4.

One approach to correct for this dead time is to measure the impact on a randomly generated signal that has a constant average rate, such as the gamma line of a radioisotope in the room. These radioisotopes should exist regardless of the activation of material from the neutron beam. Four possible candidates are the 162 keV and 186 keV lines of ^{235}U from the target and the 1173-keV and 1332-keV lines from ^{60}Co . As mentioned earlier, there is a very large background contribution from ^{60}Co from the measurement room. The 162-keV line was rejected because there was a secondary peak on the low-energy side that created problems extracted a reliable fit. Likewise, the 186-keV line was rejected because of a possible secondary peak that made the fits unreliable. Figure 3-2 shows the relative number of counts of the 186, 1173 and 1332-keV lines for various time bins. One can see that the 1173 and 1332-keV lines track each other well, while the 186-keV line varies significantly. From these results, the average of the number of counts of the 1173 and 1332-keV gamma-lines was used to determine the effective live time of the various time bins.

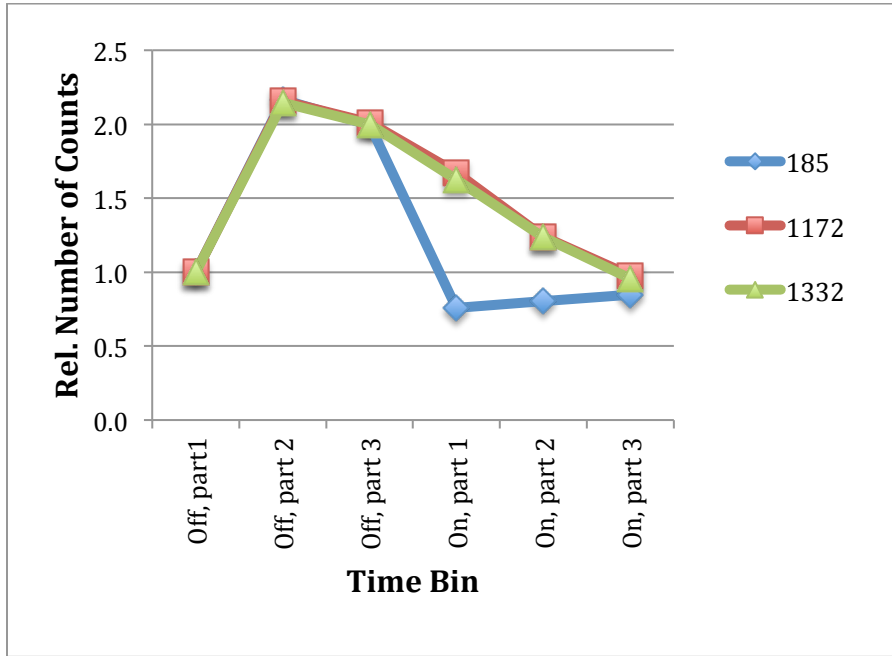


Figure 3-2: Relative number of counts per time bin for possible gamma lines that could be used to determine the effective live time of the time bin. “Off” and “On” refer to beam off and beam on, respectively.

4.0 Analysis

4.1 Time Dependence

The critical characteristic for a viable signature of ^{235}U isomer or related fission product will be the time dependence over the beam cycle. The signature will behave differently for the beam-on and beam-off periods. For the beam-on period, the signature rate will increase as the parent state is populated and decays. For the beam-off period, the signature rate will exponentially decay. Analytically, it should follow the form:

$$N(t) = \begin{cases} \frac{\beta}{\lambda}(1 - e^{-\lambda t}) + \alpha & \text{for } t \leq t_1 \\ \frac{\beta}{\lambda}(1 - e^{-\lambda t_1})e^{-\lambda(t-t_1)} + \alpha & \text{for } t > t_1 \end{cases} \quad (1)$$

where β is related to the cross section of the process, λ is related to the decay of the state, and α is an arbitrary factor, and t_1 is the time the beam turns off. All three parameters, α , β and λ , are fit parameters. An example of this form is shown in Figure 4-1, where $\alpha = 0$, $\beta = 0.1$ and λ corresponds to a $10 \mu\text{s}$ half-life. Note that there remains a small but noticeable amount of count rate at the end of the beam off

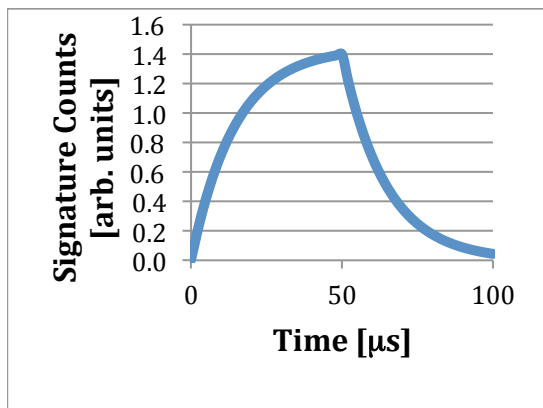


Figure 4-1: Time Distribution of gamma signature with 10 μs half-life. Note that the first 50 μs corresponds to beam on, while the latter to beam-off.

fell into a specified time bins. There were six equally sized time bins, three for beam on and three for beam off. The gamma peaks were then fit for each of the all time bins. The effective live time of the time bins was corrected by using the average intensity of the 1172 and 1332-keV lines. The live-time corrected counts for each bin for a given gamma line were then fit to each of the three forms to determine the χ^2 per degree of freedom (DOF) to identify the functional form that best fit the data.

4.2 Gamma Peak Fit Procedure

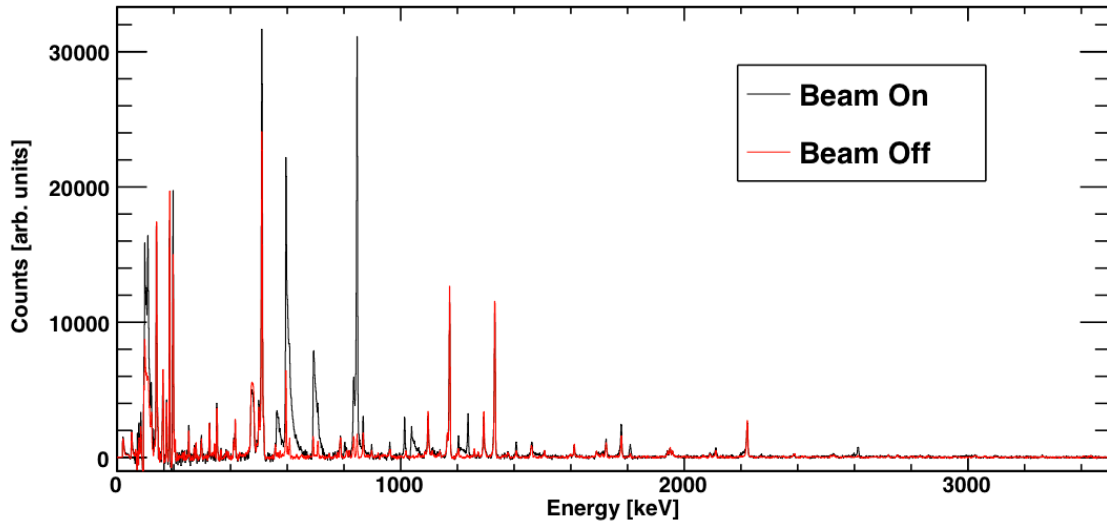
It was necessary to determine the strength of the gamma lines for each of the six time bins in a manner that would enable a direct comparison across the time bins. A comparison of the beam-on and beam-off spectra is shown in Fig. 4-2. The spectra for each of the six time bins were fit following the same procedure. First the continuum background was subtracted from the spectrum. Next, the peaks in small energy windows were fit to a simple Gaussian. Multiple peaks within the same window were fit simultaneously, so that multiplets could easily be fit simultaneously. The width of the peaks was constrained to a linear function of energy determined by prior fits to a variety of peaks in the spectrum. The background in each window was fit to a linear function. The process was done iteratively until the residual of the fit no longer contains any significant peaks.

An example of the results of the fitting process is shown in Fig. 4-3. The residual of the fit to the background continuum spectrum reveals some interesting characteristics of the fitting procedure. The non-Gaussian shapes like the ~ 700 -keV saw tooth inelastic germanium peak must be fit using multiple Gaussians. This approach does not fit the spectrum well, but because the saw tooth peak is by definition uninteresting this poor performance does not impact the results. The oscillations of the residue under the peaks suggests that the peaks are not quite Gaussian, which is quite likely given that the spectrum is generated by combining the results of four different detectors. Because the fit was conducted using least squares minimization, the fit will maintain the area under the peak while sacrificing the bin-for-bin match of the fit to the data [Bevington, 2003]. Thus, the oscillations in the residue should cancel out so that the area under the curve of the fit should well match the area under the peak for the measured spectrum.

period. This will effectively wrap around to the next beam on period. This wrap-around issue is one reason for the addition of the α term in the functional form.

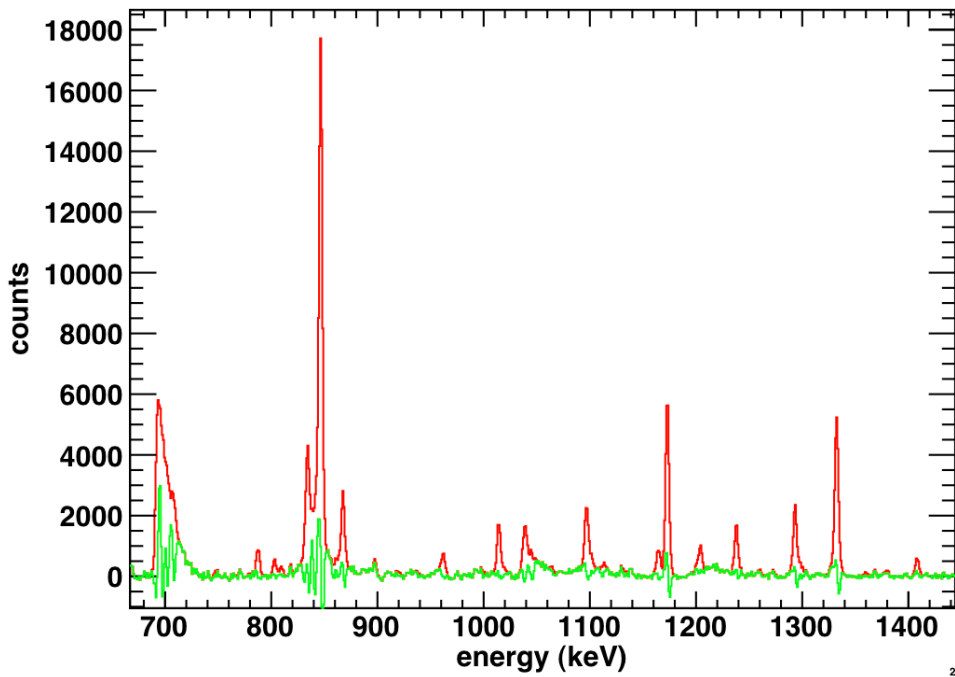
There are two other basic shapes that one will see. First, there will be a step function that is high while the beam is on and low when the beam is off. This time distribution can occur for signatures that occur only when the beam is on, like the 846-keV line from inelastic neutron scattering on ^{56}Fe . This structure will also occur for signatures that have a very short half, $t_{1/2} < 2 \mu\text{s}$. The second type of time distribution is flat. This type of time distribution will be generated by gamma rays from isotopes in the room background or from the HEU itself, or by time dependent signatures that have a long half-life, $t_{1/2} > 50 \mu\text{s}$.

To identify the time structure of various gamma lines, we created histograms of the energy in which the even



2011-06-28 17:4

Figure 4-3: Comparison of continuum subtracted gamma spectrum for beam on and beam off.



2011-06-29 10:30:13

Figure 4-2: Example of results of fitting process. The red line is the continuum background subtracted spectrum, while the green line is the residue of the fit.

4.3 Time Structure Identification

Many of the observed gamma lines were attributed to a variety of origins in [Warren, 2010]. Our analysis identified several different lines in both the beam-on and beam-off time windows. A list of those lines and their identified time structure is shown in Table 4-1. In the table, an “*” indicates the most likely evaluation on the possible structure, however the evaluation is no certain. “Small” indicates that the time-binned peaks did not have adequate statistics to make an unambiguous evaluation. The 897.7-keV peak did not appear to follow any of the anticipated time structures.

We identified two candidate peaks. The time structure of these two candidates is shown in Fig. 4-4. A plot of the spectrum for beam on and beam off for both candidates is shown in Fig. 4-5. The statistically weaker candidate is at 1164.9 keV. The χ^2/DOF for the decay structure is 2.5, but for a constant function it is 6.7. The separation in quality of fit is not significant enough to label this peak as a signature

Table 4-1: Time Structure of Previously Unidentified Lines. See text for description

Energy (keV)	Time Structure
252.5	Flat*
277.9	Flat
367.3	Flat
492.6	Flat*
516.6	Flat
830.7	Step
897.7	Indeterminate
1164.9	Decay*
1204.7	Decay
1378.8	Flat
1611.9	Flat
1690.7	Flat
1696.6	Flat
1718.8	Step
1724.3	Flat
1941.6	Flat
1950.2	Flat
1958.3	Flat
2090.6	Step*
2719.3	Small
2830.9	Small
2862.5	Small
3025.9	Small
3100.0	Small
3264.7	Small

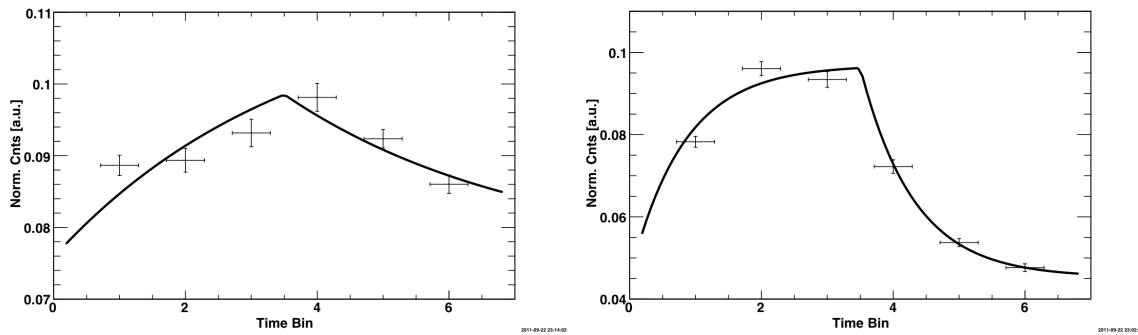


Figure 4-4: Time distributions of candidate peaks, along with decay time structure fit. The left plot is for 1164-keV peak and the right plot is for the 1204-keV peak. Each time bin is approximately 16.7 μ s wide.

unambiguously. The decay constant of the fit suggests that if the 1164-keV is due to decay, it has a half-life of $42 \pm 9 \mu$ s.

The second candidate is at 1204.7 keV. Although not identified in [Warren, 2011] as a germanium excitation, this line is identified as a thermal neutron capture line [CapGam] and an inelastic neutron scattering line for $^{74}\text{Ge}(n,n')$ [Heusser, 1993]. As a check on the time dependence of the 1204-keV peak, a well-known strong germanium excitation at 867 keV was examined and found to have a similar time structure.

There are several possible explanations for the observed 1164-keV peak. Each of these is discussed below:

- Decay of a fission product: A search of the online Table of Radioactive Isotopes database [TORI, 1999] did not real any fission products with half-lives between 35 and 50 μ s.
- Neutron capture in the germanium detector: There are no germanium-related neutron capture gamma rays within ± 1 keV of the 1164-keV peak.
- Neutron inelastic scattering photon in the germanium detector: A strong gamma ray from neutron inelastic scattering would likely have been listed in [Heusser-1993] and would likely also appear as a neutron capture gamma ray. However, it appears in neither.
- Neutron capture or inelastic scattering in the iron of the sample. There is one line gamma-line related to ^{57}Fe in [CapGam], although it has several stronger associated gamma-lines that are not observed. There is no 1164-keV gamma ray for the transitions of ^{56}Fe listed in [NuDat 2.5]. As a result, the 1164-keV gamma ray is no likely a gamma-ray related to neutrons on iron.
- Room background: The 1164-keV peak does not appear in the room background measurement with beam off,
- Isomeric transition of ^{235}U : One can conclude that the 1164-keV peak is related to the isomeric transition of ^{235}U only if all possible other explanations have been rejected and the time structure of the peaks is statistically significant.

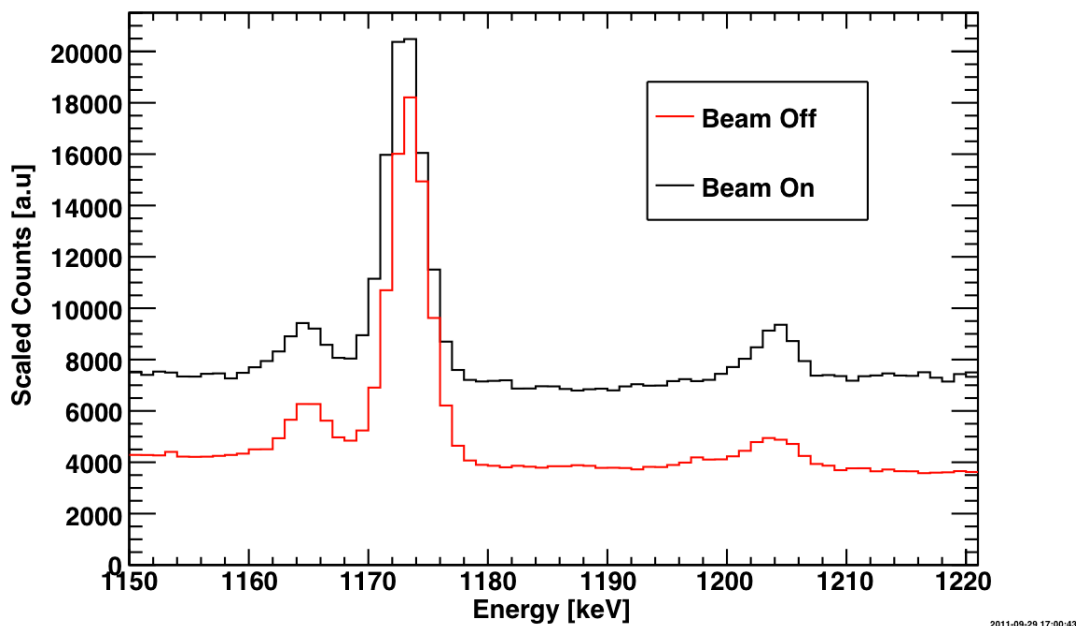


Figure 4-5: Energy Spectra for beam on and beam off for the two possible candidates identified in the time structure analysis. The beam off spectra (red) has been scaled to so that the counts in the 1173-keV peak of the two spectra are the same.

Through the process of elimination, the most likely explanation for the 1164-keV peak is that it is an indication of an isomeric state of ^{235}U . However, the statistical significance of the measurement prevent the authors from declaring this as an unambiguous isomeric signature

5.0 Conclusion

The project has completed analysis of the December 2010 experiment at LBNL. The time structure of a variety of gamma-ray peaks was studied to determine the possible origin of the gamma rays. Three basic time structures were considered. A flat time distribution was related to room or target background. A step function dependence that was high for beam on and low for beam off was considered to be a beam-related background. It is possible that isomer and fission product signatures with short half-lives, less than a few μs , could appear as step functions in the time-binned data. The decay time structure accounts for the growing-in of the decay as neutrons hit the target as well as the radioactive decay of the state.

There was one candidate, at 1164.9 ± 0.3 keV, of an isomeric signature of ^{235}U . The half-life of the state is estimated to be 42 ± 9 μs . Alternative explanations for the 1164-keV gamma ray have been investigated and found invalid. Unfortunately, the relatively limited statistics of the measurement restrict the authors to labeling the 1164-keV gamma ray as a candidate for isomeric transition in ^{235}U . Further measurements may reveal that the time structure does follow the decay time structure for a ~ 42 μs half-life decay, in which case the gamma-ray could be used to identify ^{235}U using neutron scattering. It will be necessary to repeat the measurements to achieve higher statistics better systematics before the 1164-keV line can be confirmed as a signature of isomeric decay of ^{235}U .

6.0 References

- [Bevington, 2003] Bevington, PR and DK Robinson, 2003. "Data Reduction and Error Analysis for the Physical Sciences." Third Edition, McGraw Hill, Boston.
- [CapGam] Thermal Neutron Capture γ 's (CapGam), National Nuclear Data Center, <http://www.nndc.bnl.gov/capgam/index.html>.
- [Heusser, 1993] G. Heusser, "Cosmic ray-induced background in Ge-spectrometry," Nucl. Inst. Meth. B83, 223-228 (1993).
- [NuDat 2.5] NuDat 2.5, National Nuclear Data Center, Brookhaven National Laboratory, <http://www.nndc.bnl.gov/nudat2/>.
- [Ressler, 2009] Ressler, JJ, JA Caggiano, and GA Warren. 2009b. *Annual Progress Report for Actinide Isomer Detection (2009)*. Report No. PNNL-18868, Pacific Northwest National Laboratory, Richland, WA.
- [Ressler, 2010] Ressler, JJ, et al. 2010. "Fission Fragment Isomers Populated Via ${}^6\text{Li}+{}^{232}\text{Th}$." *Physical Review C* 81(1):014301.
- [TORI, 1999] S.Y.F. Chu, L.P. Ekstroem, R.B. Firestone, "The LUND/LBNL Table of Radioactive Isotopes, Version 2.0, February 1999", <http://nucleardata.nuclear.lu.se/NuclearData/toi/>.
- [Warren, 2011] Warren, GA, CJ Francy, JJ Ressler, LE Erikson, EA Miller, and R Hatarik. 2011. [FY2010 Annual Report for the Actinide Isomer Detection Project](#) . PNNL-20145, Pacific Northwest National Laboratory, Richland, WA.



Pacific Northwest
NATIONAL LABORATORY

*Proudly Operated by **Battelle** Since 1965*

902 Battelle Boulevard
P.O. Box 999
Richland, WA 99352
1-888-375-PNNL (7665)

www.pnl.gov



U.S. DEPARTMENT OF
ENERGY